Molecular Therapy
Oncolytics
Original Article

miR-1207-5p suppresses laryngeal squamous cell carcinoma progression by downregulating SKA3 and inhibiting epithelial-mesenchymal transition

Yongyan Wu,[1,2,3,4,6] Fengsheng Dai,[2,6] Yuliang Zhang,[2,6] Xiwang Zheng,[1,2] Li Li,[5] Yu Zhang,[3] Jimin Cao,[3] and Wei Gao[1,2,3,5]

[1]General Hospital, Clinical Medical Academy, Shenzhen University, Shenzhen 518055, Guangdong, China; [2]Shanxi Key Laboratory of Otorhinolaryngology Head and Neck Cancer, Shanxi Province Clinical Medical Research Center for Precision Medicine of Head and Neck Cancer, First Hospital of Shanxi Medical University, Taiyuan 030001, Shanxi, China; [3]Key Laboratory of Cellular Physiology, Ministry of Education, Shanxi Medical University, Taiyuan 030001, Shanxi, China; [4]Department of Biochemistry & Molecular Biology, Shanxi Medical University, Taiyuan 030001, Shanxi, China; [5]Department of Cell biology and Genetics, Basic Medical School of Shanxi Medical University, Taiyuan 030001, Shanxi, China

Laryngeal squamous cell carcinoma (LSCC) is the second most common head and neck cancer. Previously, we discovered that miR-1207-5p was downregulated in LSCC. In this study, the clinical significance, function, and mechanism of miR-1207-5p in LSCC were investigated. Downregulation of miR-1207-5p was found to be strongly linked to the malignant progression of LSCC. Functional studies revealed that miR-1207-5p upregulation suppressed LSCC cell proliferation, invasion, migration, and xenograft tumor growth. Bioinformatics analysis revealed that miR-1207-5p target genes were involved in cell cycle regulation, proliferation, adhesion, and the phosphatidylinositol 3-kinase (PI3K)/Akt pathway. Mechanistic studies revealed that miR-1207-5p interacts directly with the 3′ untranslated region of spindle and kinetochore associated complex subunit 3 (SKA3) and downregulates SKA3 expression. Furthermore, SKA3 was found to be overexpressed in LSCC, and its high expression was associated with tumor progression and a poor prognosis. Rescue experiments demonstrated that miR-1207-5p inhibited the malignant phenotypes of LSCC via SKA3. Furthermore, miR-1207-5p upregulation or knockdown of SKA3 inhibited the epithelial-mesenchymal transition (EMT). Collectively, miR-1207-5p inhibited LSCC malignant progression by downregulating SKA3 and preventing EMT. These findings provide new insights into the mechanism of LSCC progression, as well as new potential biomarkers and therapeutic targets for LSCC diagnosis and treatment.

INTRODUCTION

The global incidence of laryngeal squamous cell carcinoma (LSCC) is gradually increasing.[1,2] LSCC has a negative impact on patients' quality of life because it impairs their ability to breathe, swallow, and speak.[3] Despite advances in comprehensive LSCC treatment, the 5-year survival rate has not decreased significantly in decades.[4] The main risk factors for a poor prognosis of LSCC are invasion and metastasis of cervical lymph nodes.[5] Furthermore, the diagnostic delay caused by the absence of obvious symptoms in the early stage is an unfavorable factor for LSCC prognosis.[6] Several risk factors such as smoking, alcohol consumption, and human papillomavirus (HPV) have been implicated in the pathogenesis of laryngeal cancer.[2,7] However, the molecular mechanism of LSCC tumorigenesis, invasion, and metastasis, on the other hand, remains unknown.[8] Furthermore, based on a large number of clinical samples, several potential biomarkers for LSCC diagnosis have been identified, including mRNA, circular RNA (circRNA), long non-coding RNA (lncRNA), as well as microRNA (miRNA).[5,9–12] Unfortunately, no biomarkers are currently available for clinical diagnosis of LSCC. Understanding the mechanism of LSCC progression, invasion, and metastasis, as well as identifying more reliable biomarkers, is therefore critical for LSCC diagnosis and treatment.

miRNAs are non-coding endogenous RNA molecules made up of 18–22 nucleotides that primarily dock the 3′ untranslated region (UTR) of a target mRNA, causing degeneration or translation suppression.[13] miRNAs have been implicated in the pathogenesis of various tumors, as well as regulating cell proliferation, invasion, migration, chemoresistance, and angiogenesis, via multiple signaling pathways.[14,15] Abnormal miRNA expression can lead to aberrant expression of oncogenes or tumor suppressor genes, enhancing cancer initiation and progression.[16,17] By directly decreasing suppressor of cytokine signaling 2 (SOCS2) expression, miR-196b can increase the invasive

Received 7 April 2021; accepted 12 August 2021;
https://doi.org/10.1016/j.omto.2021.08.001.

[6]These authors contributed equally

Correspondence: Wei Gao, MD, Shanxi Key Laboratory of Otorhinolaryngology Head and Neck Cancer, Shanxi Province Clinical Medical Research Center for Precision Medicine of Head and Neck Cancer, First Hospital of Shanxi Medical University, Taiyuan 030001, Shanxi, China.
E-mail: gaoweisxent@sxent.org
Correspondence: Jimin Cao, MD, Key Laboratory of Cellular Physiology, Ministry of Education, Shanxi Medical University, Taiyuan 030001, Shanxi, China.
E-mail: caojimin@126.com

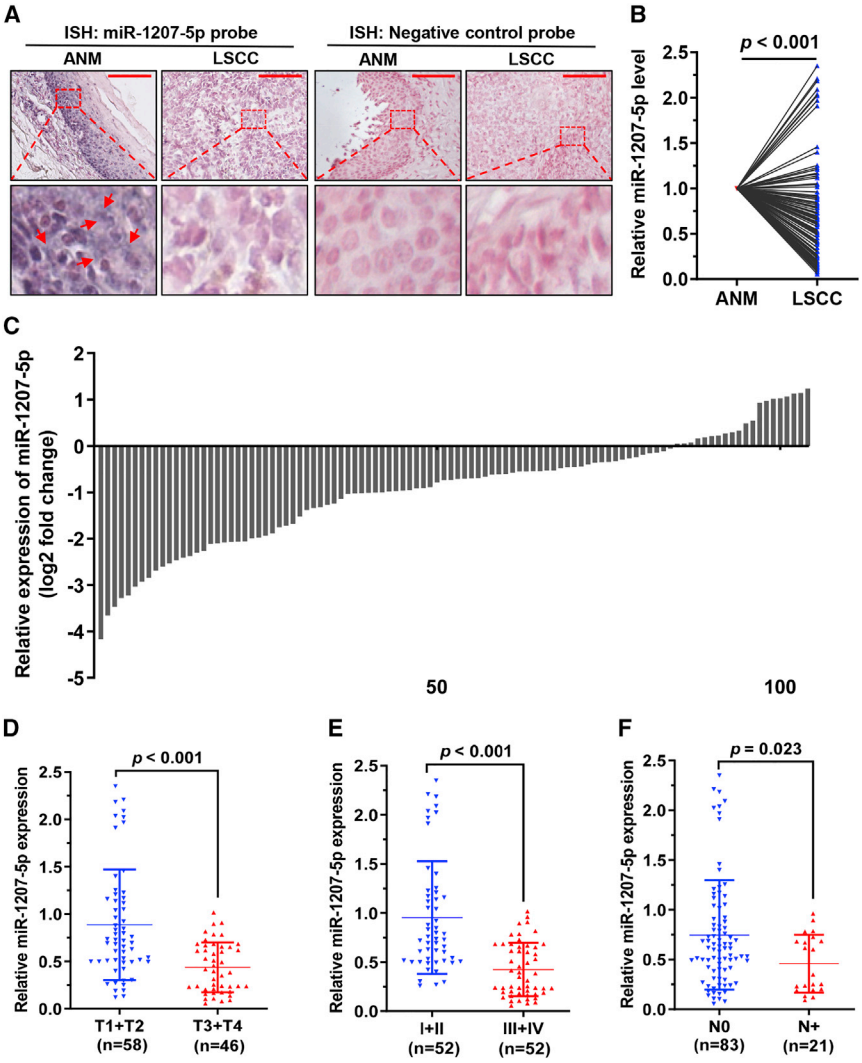

Figure 1. miR-1207-5p is downregulated in LSCC and is related to clinical features

(A) miR-1207-5p level in LSCC and matched ANM tissues was detected by *in situ* hybridizations. The red arrow indicates the miR-1207-5p signal (blue). Scale bars, 50 μm. (B and C) The expression levels of miR-1207-5p in 104 LSCC and matched ANM tissues were detected by qPCR. (D–F) Correlation assessment of miR-1207-5p levels and T stages (D), clinical stages (E), and lymph node metastasis (F).

and proliferative ability of LSCC cells while suppressing apoptosis,[18] whereas high levels of miR-1205 inhibit the growth, migratory, and invasive abilities of LSCC cells.[19] These findings suggest that miRNAs play an important role in the progression of LSCC.

Using microarray analysis, we previously identified differentially expressed genes (DEGs) in LSCC tissues and corresponding healthy mucosa (adjacent normal mucosa [ANM]) tissues. The microarray data revealed that miR-1207-5p expression is lower in LSCC tissues compared to ANM tissues, and network analysis revealed that miR-1207-5p is a central node in the LSCC transcription regulatory network.[20] In this study, we evaluated the expression and clinical value of miR-1207-5p in a large cohort of LSCC samples. The findings confirmed the under-expression of miR-1207-5p in LSCC tissues and that low expression of miR-1207-5p was associated with clinical features of LSCC. Furthermore, our findings showed that miR-1207-5p overexpression inhibited LSCC cell proliferation, invasion, and migration *in vitro* and *in vivo*. miR-1207-5p was also discovered to repress the malignant phenotypes of LSCC cells by binding to the spindle and kinetochore associated complex subunit 3 (SKA3) 3′ UTR and suppressing SKA3 expression. These findings suggested that miR-1207-5p and SKA3 are potential biomarkers and targets for LSCC diagnosis and treatment.

RESULTS

Downregulation of miR-1207-5p is linked to malignant progression of LSCC

Previous microarray data showed that miR-1207-5p was under-expressed in LSCC tissues compared to ANM tissues.[20] *In situ* hybridization was used to demonstrate the expression of miR-1207-5p in LSCC and paired ANM tissues. MiR-1207-5p expression was found to be lower in LSCC tissues compared to ANM tissues (Figure 1A). Following that, qRT-PCR was performed to determine the levels of miR-1207-5p in 104 LSCC and matched ANM tissues. The findings confirmed that miR-1207-5p was significantly and frequently under-expressed in LSCC tissues compared to paired ANM tissues (Figures 1B and 1C). A comparison of miR-1207-5p levels to clinical features of LSCC revealed that a low miR-1207-5p level was strongly associated with advanced T stage and clinical stage (Figures 1D and 1E). A low level of miR-1207-5p, in particular, was strongly linked to lymph node metastasis (Figure 1F). These findings suggested that the downregulated miR-1207-5p may play important roles in the progression of LSCC.

miR-1207-5p represses the invasion, migration, and proliferation of LSCC cells

To investigate the roles of miR-1207-5p in LSCC, we transfected miR-1207-5p mimics (miR-1207-5p) and negative control mimics (NC mimics) into the LSCC cell lines TU-177 and FD-LSC-1. After miR-1207-5p mimic transfection (Figure 2A), qPCR confirmed that miR-1207-5p was overexpressed compared to the NC arm. The CCK8 assay revealed that miR-1207-5p overexpression inhibited the proliferation of TU-177 and FD-LSC-1 cells (Figure 2B). Colony formation assays revealed that the colony formation capacity was

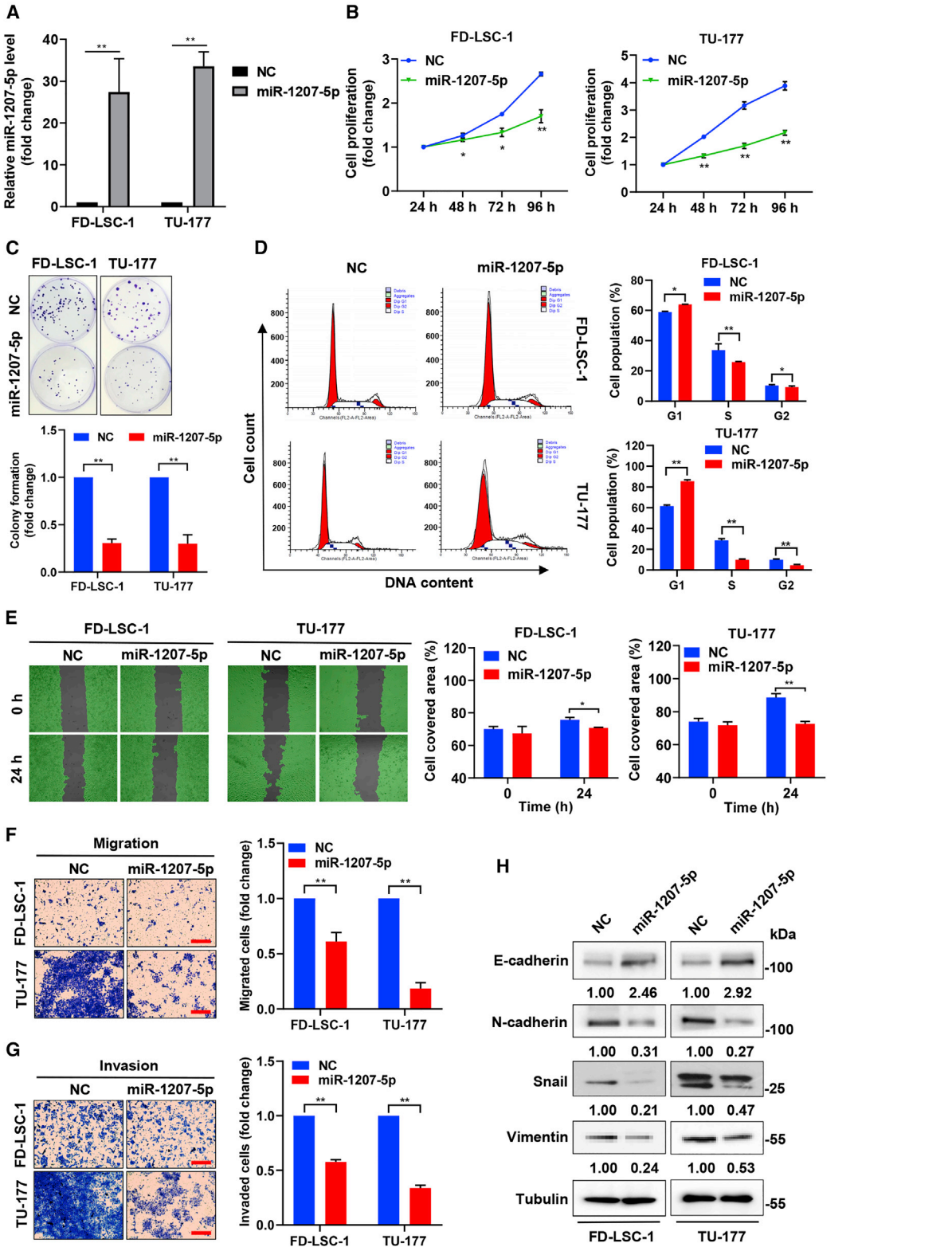

(legend on next page)

reduced in the miR-1207-5p-overexpression arm (Figure 2C). Cell cycle analysis revealed that the miR-1207-5p mimics arm had a significant accumulation of cells in the G1 phase, whereas the cell numbers in the S and G2 phases were lower (Figure 2D), indicating that miR-1207-5p suppressed LSCC cell growth by inducing G1 phase arrest.

The impact of miR-1207-5p on LSCC cell migration and invasion was then investigated. Scratch-wound healing experiments and Transwell assays indicated that higher levels of miR-1207-5p inhibited the migration ability of TU-177 and FD-LSC-1 cells (Figures 2E and 2F). Furthermore, the invasion ability of LSCC cells overexpressing miR-1207-5p was significantly reduced (Figure 2G). The epithelial-mesenchymal transition (EMT) plays an important role in tumor cell metastasis.[21] We investigated whether miR-1207-5p affects EMT in LSCC cells. Western blot analysis revealed that E-cadherin expression increased whereas Snail, N-cadherin, and Vimentin expression decreased in TU-177 and FD-LSC-1 cells transfected with miR-1207-5p mimics (Figure 2H), indicating that miR-1207-5p overexpression inhibits EMT in LSCC cells. These results highlighted the importance of miR-1207-5p in regulating LSCC cell cycle progression, invasiveness, migration, and proliferative abilities.

miR-1207-5p directly targets Spindle and kinetochore associated complex subunit 3 in LSCC cells

TargetScan was used to predict miR-1207-5p target genes, and 3,028 genes (Table S3) were obtained. Venn analysis was used to identify common genes among predicted miR-1207-5p target genes and upregulated genes in LSCC tissue microarray and RNA sequencing (RNA-seq) data[10] (Tables S4 and S5), and 70 intersected genes were obtained (Figure 3A; Table S6). Gene Ontology (GO) analysis revealed that the intersection genes were involved in the biological processes of chromosome segregation, positive regulation of mitotic exit, cell proliferation, sister chromatid cohesion, collagen fibril organization, mitotic nuclear division, cell division, cell adhesion, and mitotic cell cycle G1/S transition (Figure 3B; Table S7). Kyoto Encyclopedia of Genes and Genomes (KEGG) pathway analysis revealed that miR-1207-5p candidate target genes were enriched in extracellular matrix (ECM)-receptor interaction, focal adhesion, and the phosphatidylinositol 3-kinase (PI3K)-Akt signaling pathway (Figure 3C; Table S7). These findings suggested that miR-1207-5p may affect the LSCC phenotype by regulating these target genes and related pathways.

Given that miR-1207-5p is involved in cell cycle regulation, we focused on candidate target genes involved in cell cycle regulation. SKA3 is a critical component of the SKA complex, which is required for normal chromosome segregation and cell division.[22] Therefore, we hypothesized that *SKA3* is a direct target of miR-1207-5p. To test this hypothesis, qPCR and western blot were used to determine the expression of SKA3 in LSCC cells transfected with miR-1207-5p mimics. The results showed that miR-1207-5p overexpression decreased SKA3 levels (Figures 3D and 3E). Furthermore, luciferase reporter assays revealed that wild-type (WT) *SKA3* 3′ UTR luciferase activity was significantly reduced in cells expressing miR-1207-5p, whereas mutant (Mut) *SKA3* 3′ UTR luciferase activity showed no significant change (Figure 3F). In contrast, miR-1207-5p inhibitor transfection increased the luciferase activity of the WT *SKA3* 3′ UTR reporter (Figure 3F). These findings show that *SKA3* is a direct target of miR-1207-5p.

Upregulation of SKA3 is linked to tumor progression and poor disease outcomes in LSCC

SKA3 is involved in tumor cell growth and migration in hepatocellular carcinoma (HCC) and cervical cancer.[23,24] SKA3 levels were determined by qPCR in 150 LSCC tissues and matched ANM tissues. SKA3 was found to be upregulated in LSCC tissues (Figure 4A). Correlation analysis revealed that a high SKA3 level was positively related to T and N stages, as well as the clinical stage (Figures 4B–4D). Furthermore, a high SKA3 level was also found to be strongly associated with poor pathological LSCC differentiation (Figure 4E). The SKA3 protein level in LSCC tissues was confirmed with immunohistochemical (IHC) staining and western blotting, and the results showed a higher SKA3 protein level in LSCC tissues than in ANM tissues (Figures 4F and 4G). The The Cancer Genome Atlas (TCGA) repository data revealed that SKA3 expression was higher in LSCC and head and neck squamous cell carcinoma (HNSCC) (Figure 4H), and Kaplan-Meier analysis showed that HNSCC patients with high levels of SKA3 had a poor survival time (Figure 4I). Analysis of the TCGA data revealed that SKA3 was upregulated in 18 types of cancer, including HNSCC (Figure 4J). Kaplan-Meier analysis revealed that high SKA3 levels were significantly related to poor survival time in 32 types of cancer other than HNSCC (Figure 4K).

SKA3 knockdown inhibits the invasion, migration, and proliferation of LSCC cells

To investigate the effects of SKA3 on LSCC cells, the SKA3 level was knocked down by specific small interfering RNAs (siRNAs) (Figure 5A). CCK8 and the colony formation assays showed that SKA3 knockdown inhibited the proliferative and colony-forming ability of LSCC cells (Figures 5B and 5C). Interestingly, SKA3 knockdown

Figure 2. miR-1207-5p upregulation represses cell cycle progression, migration, invasion, and proliferation of LSCC cells

(A) LSCC cells were transfected with miR-1207-5p or negative control (NC) mimics via transfection, and the miR-1207-5p level was validated by qPCR. (B) The proliferation of miR-1207-5p or negative control (NC) mimics transfected cells was determined by CCK8 assay at the time points indicated. (C) Analysis of colony formation of miR-1207-5p overexpressed LSCC cells. (D) Cells transfected with miR-1207-5p mimics and then cell cycle analysis by flow cytometry. (E) Cells transfected with miR-1207-5p or NC mimics and wound healing assay at the time points indicated. (F and G) Cells transfected with miR-1207-5p or NC mimics and migration as well as invasion ability determined by Transwell assays. (H) Cells transfected with miR-1207-5p or NC mimics for 48 h, and the levels of E-cadherin, Snail, Vimentin, and N-cadherin proteins were determined by western blotting. Protein bands were quantified by ImageJ, and the relative expression was calculated by normalizing to Tubulin and NC arm. Data are mean ± SD of three separate experiments. *$p < 0.05$ and **$p < 0.01$.

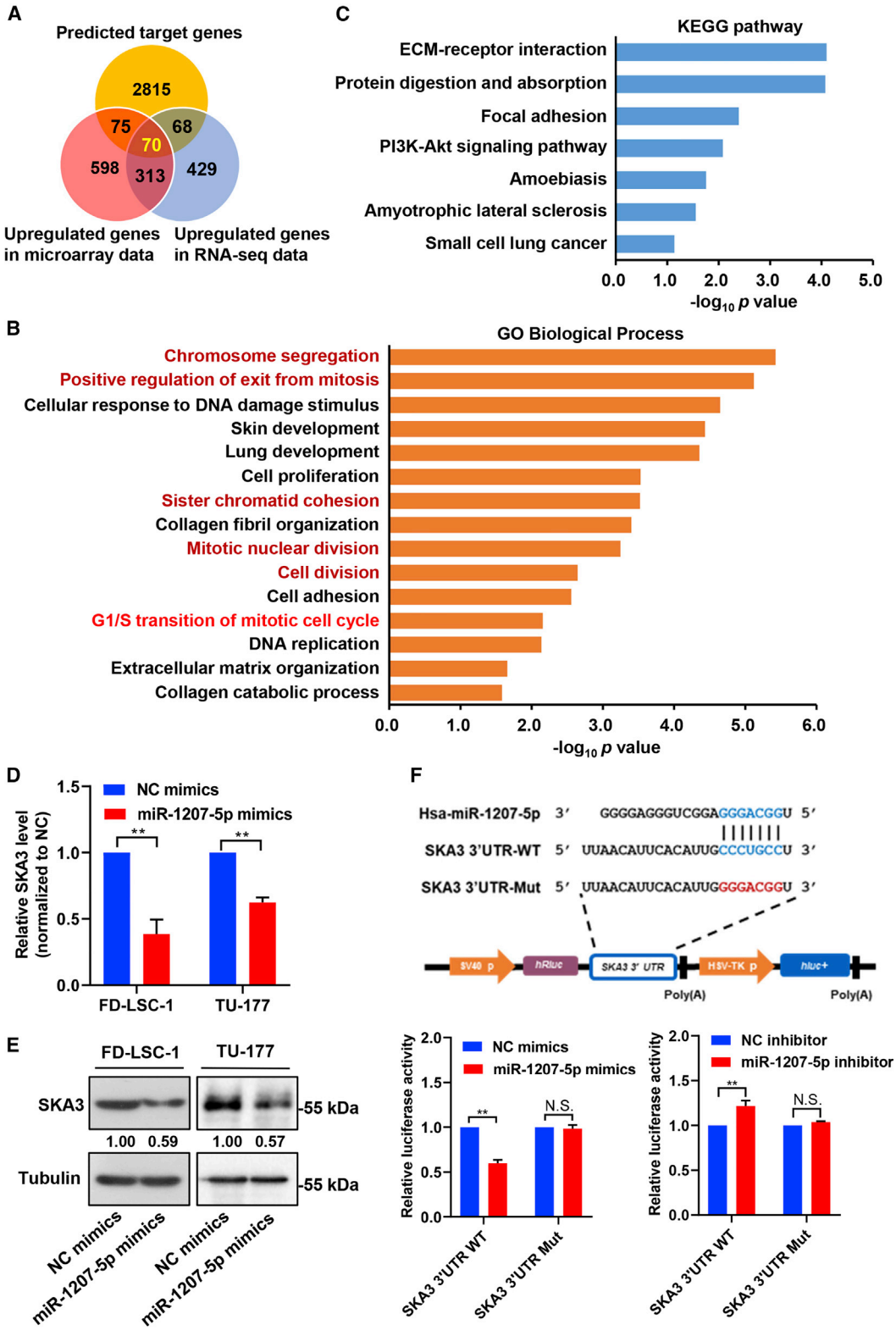

(legend on next page)

resulted in G1 phase arrest (Figure 5D). Furthermore, scratch-wound healing experiments and Transwell assays demonstrated that the loss of function of SKA3 reduced migration and invasion ability (Figures 5E–5G). Furthermore, after SKA3 knockdown, the E-cadherin protein level was upregulated whereas the N-cadherin, Snail, and Vimentin protein levels were downregulated in LSCC cells (Figure 5H). Taken together, SKA3 knockdown phenocopied the miR-1207-5p influence on LSCC cells, indicating that *SKA3* is an oncogenic gene in LSCC.

SKA3 overexpression mitigates the effects of miR-1207-5p on LSCC cell phenotypes

Rescue experiments were designed to determine whether miR-1207-5p inhibited LSCC cell malignant behavior by downregulating the target gene SKA3. TU-177 and FD-LSC-1 cells were co-transfected with miR-1207-5p mimics and the SKA3 overexpression plasmid (Figure 6A). Colony formation and CCK8 assays revealed that SKA3 upregulation reversed the reduction in colony formation and proliferative capacity of LSCC cells caused by miR-1207-5p mimics (Figures 6B and 6C). Furthermore, Transwell and scratch-wound healing assays revealed that SKA3 upregulation reversed the decrease in invasive and migration abilities caused by miR-1207-5p upregulation (Figures 6D–6F). These findings suggested that miR-1207-5p could suppress LSCC cell migration, invasion, and proliferation primarily by inhibiting SKA3 oncogenic influence.

miR-1207-5p inhibits LSCC xenograft tumor growth in a preclinical model

We investigated the effects of miR-1207-5p on LSCC *in vivo* using a xenograft tumor model. Every 2 days beginning on day 10, NC or miR-1207-5p agomir was injected into tumors, and on day 22 the mice were euthanized. The tumor growth curve revealed that the growth rate of xenograft tumors formed by TU-177 cells with high miR-1207-5p levels was significantly slowed compared to the NC arm (Figure 7A). miR-1207-5p agomir-injected xenograft tumors weighed less than those in the NC arm (Figure 7B). The qPCR assay revealed that the miR-1207-5p levels were significantly higher in miR-1207-5p agomir-injected xenograft tumors (Figure 7C). Furthermore, IHC staining revealed that the expression level of E-cadherin was increased in miR-1207-5p agomir-injected xenograft tumors compared to the NC arm, whereas the expression levels of SKA3, Ki67, N-cadherin, Snail, and Vimentin were reduced in miR-1207-5p agomir-injected xenograft tumors compared to the NC group (Figure 7D). Taken together, these findings indicated that miR-1207-5p inhibits LSCC cell growth as well as EMT *in vivo*.

DISCUSSION

miRNAs have been implicated in the pathogenesis of various cancers, specifically in their occurrence, invasion, metastasis, and chemoresistance.[25–27] Microarrays and RNA-seq were used to identify DEGs in LSCC tissues and cells.[9,28,29] Using microarrays, we recently investigated the miRNAs that were differentially expressed in LSCC tissues. According to our findings, miR-1207-5p is under-expressed in LSCC tissues and may be an important regulator in the LSCC transcription regulatory network.[20] In this study, the clinical value, functional role, and mechanism of miR-1207-5p in LSCC were explored. The findings showed that miR-1207-5p downregulation was strongly linked to the progression of LSCC malignancy. Functional studies demonstrated that miR-1207-5p suppressed the invasive, migration, and proliferative potential of LSCC cells *in vitro* and *in vivo*. miR-1207-5p interacted with the SKA3 3′ UTR and downregulated SKA3 expression. Furthermore, we found that SKA3 was upregulated in LSCC, and a high SKA3 level was associated with tumor progression and poor LSCC disease outcomes. Rescue experiments revealed that miR-1207-5p suppresses LSCC cell malignant phenotypes by targeting SKA3. Furthermore, upregulation or silencing of SKA3 by miR-1207-5p inhibited EMT.

miR-1207-5p is under-expressed in esophageal carcinoma tissues, and its overexpression reduces esophageal carcinoma invasion and increases apoptosis by inhibiting stomatin-like protein 2.[30] Furthermore, Zhao et al. found that miR-1207-5p levels were reduced in HCC cell lines and tissues and that its overexpression inhibited HCC cell proliferation and invasion via regulation of the Akt/mammalian target of rapamycin (mTOR) signaling pathway.[31] Meanwhile, miR-1207-5p inhibits liver cancer proliferation and metastasis by regulating Wnt/β-Catenin signaling.[32] Moreover, miR-1207-5p can suppress gastric cancer progression via downregulating hTERT expression[33] and suppress colorectal cancer cell migration, invasion, and proliferation by targeting FMNL2.[34] These findings suggested that miR-1207-5p acts as a tumor inhibitor, suppressing malignant behavior. miR-1207-5p, on the other hand, plays oncogenic roles in other cancers. According to Hou et al. triple-negative breast cancer cells with upregulated miR-1207-5p enhanced cell growth and resistance to taxol treatment by downregulating LZTS1 expression.[35] Yan et al. found that miR-1207-5p could promote breast cancer cell proliferation by targeting STAT6.[36] According to our findings, miR-1207-5p may be under-expressed in LSCC tissues, which may be linked to the malignant progression of LSCC. Additionally, functional studies indicated that miR-1207-5p functions as a tumor suppressor miRNA in LSCC, suppressing LSCC cell proliferation, migration, and invasion.

Figure 3. Functional annotation and experimental validation of miR-1207-5p target gene

(A) Venn evaluation of predicted miR-1207-5p target genes and upregulated genes in LSCC tissues. (B) GO assessment of candidate miR-1207-5p target genes. Top 15 biological processes plotted based on enriched gene number and p value. (C) KEGG pathway analysis of candidate miR-1207-5p target genes. (D and E) LSCC cells were transfected with miR-1207-5p or NC mimics for 48 h. Expression levels of SKA3 mRNA (D) and protein (E) were determined by qPCR and western blotting. Protein bands were quantified by ImageJ, and the relative expression was calculated by normalizing to Tubulin and NC arm. (F) FD-LSC-1 cells co-transfected with miR-1207-5p mimics/inhibitor with wild-type or mutant SKA3 3′ UTR reporter plasmid for 48 h. The relative luciferase activity was detected. Data are mean ± SD of three separate experiments. *$p < 0.05$ and **$p < 0.01$.

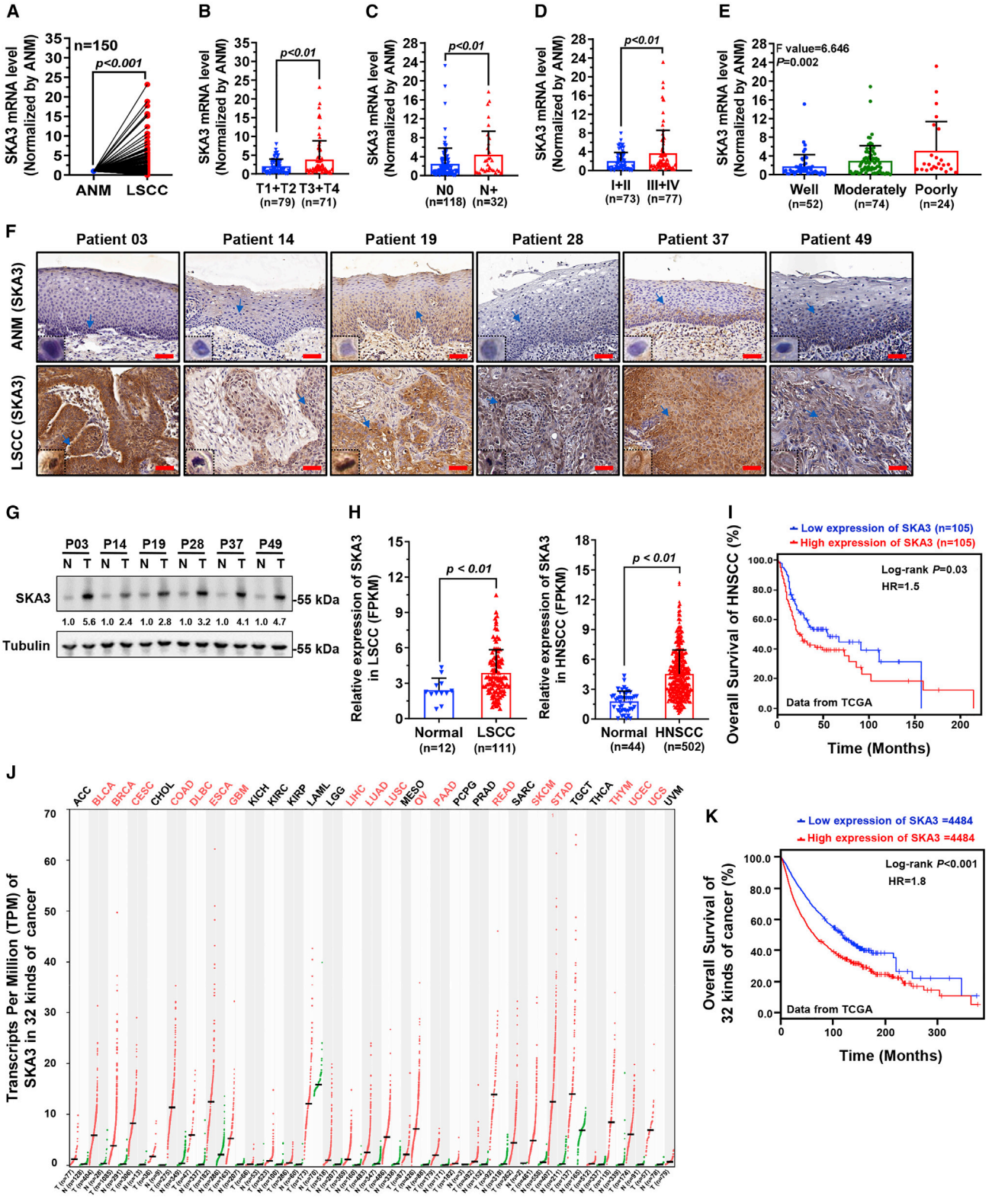

(legend on next page)

Bioinformatics analysis revealed that miR-1207-5p target genes were involved in cell cycle-related biological activities such as sister chromatid cohesion, the mitotic cell cycle's G1/S transition, and cell multiplication. The predicted miR-1207-5p target gene SKA3 is an important component of the SKA1 complex, which mediates the attachment of microtubules to kinetochores during mitosis. The SKA3 protein is released to the outer kinetochore and is required for normal chromosome segregation and subsequent cell division.[22,37,38] Recent research indicates that SKA3 knockdown causes cell cycle arrest and apoptosis in hepatocellular carcinoma (HCC) cells.[23] Consistently, we found that overexpression of miR-1207-5p or SKA3 knockdown causes cell cycle arrest in LSCC cells.

EMT is closely associated with cancer metastasis and progression.[39,40] At the molecular level, EMT is characterized by the upregulation of vimentin, N-cadherin, and snail and downregulation of E-cadherin.[41] When miR-1207-5p was overexpressed or SKA3 was knocked down, E-cadherin was increased. N-cadherin, Snail, and Vimentin levels, on the other hand, decreased. These findings suggest that miR-1207-5p and its target SKA3 influence LSCC progression and metastasis via EMT. Numerous studies have shown that activation of the PI3K/Akt signaling pathway promotes EMT, proliferation, invasion, and migration in various types of cancer.[42–45] Furthermore, overexpression of SKA3 has been shown to activate the PI3K/Akt signaling pathway in cervical cancer and lung adenocarcinoma.[24,46] Recently, we discovered that SKA3 activates the PI3K/Akt pathway by binding to and stabilizing polo-like kinase 1 (PLK1).[8] Therefore, our findings indicated that miR-1207-5p functions as a tumor suppressor by downregulating SKA3, and the PI3K/Akt pathway is an important downstream target responsible for miR-1207-5p/SKA3-mediated phenotypes, at least in part.

Furthermore, the *in vivo* assay results confirmed that miR-1207-5p overexpression inhibited LSCC xenograft tumor growth and EMT by downregulating SKA3. miR-1207-5p agomir was directly injected into the tumor in preclinical model experiments, as previously reported,[47] and we found that tumor growth was significantly retarded. This method, in particular, increased the clinical significance of miR-1207-5p for LSCC therapy.

In conclusion, the current study found that miR-1207-5p functions as a novel tumor suppressor in LSCC. *In vitro* and *in vivo* experiments demonstrate that miR-1207-5p downregulates SKA3 to inhibit proliferation, migration, and invasion (Figure 7E). Furthermore, a low miR-1207-5p level or a high SKA3 level was associated with the malignant progression of LSCC, implying that both miR-1207-5p and SKA3 could be used as biomarkers for LSCC diagnosis. *In vivo* experiments with miR-1207-5p agomir explored the possibility of using miRNA as a molecular drug for LSCC treatment. Therefore, miR-1207-5p upregulation and SKA3 silencing should be considered as potential therapeutic strategies in the future.

MATERIALS AND METHODS

Ethical statement and tissue samples

This study was approved by the Research Ethics Committee of Shanxi Medical University. The Animal Care Commission of Shanxi Medical University's Experimental Animal Center approved the protocol used to conduct animal experiments. Great care was taken to minimize the suffering of the included animals. LSCC and ANM tissue samples were obtained from patients admitted for surgery at the First Hospital of Shanxi Medical University's Department of Otolaryngology-Head and Neck Surgery. The patients were not subjected to radiotherapy or chemotherapy before surgery. All patients signed informed consent.

Cell culture

The FD-LSC-1 cell line (provided by Professor Zhou's lab[48]) was maintained in bronchial epithelial cell growth medium (BEGM) (Lonza, Walkersville, MD, USA) supplemented with 10% fetal bovine serum (FBS) (BI, Cromwell, CT, USA). The TU-177 cells were purchased from Bioleaf Biotech (Shanghai, China) and maintained in minimum essential medium (MEM) supplemented with 10% FBS (BI).

Plasmid construction and transfection

To construct the *SKA3* 3′ UTR luciferase reporter vector, the WT *SKA3* 3′ UTR sequence was obtained by RT-PCR using FD-LSC-1 cDNA as template, and the miR-1207-5p binding site mutated 3′ UTR sequence was obtained by overlap extension PCR and the resulting fragments were cloned into the psiCHECK-2 vector. The full length of the *SKA3* coding sequence was cloned into the p3FLAG-CMV-10 vector for SKA3 overexpression plasmid construction. Plasmid transfection was conducted with the Lipofectamine 3000 reagent (Thermo Fisher Scientific) according to the manufacturer's protocol.

miRNA mimics, miRNA inhibitor, miRNA agomir, and siRNA

NC mimics, miR-1207-5p mimics, miR-1207-5p agomir, siRNA targeting *SKA3* (si-SKA3), and negative oligos (si-NC) were obtained from GenePharma (Shanghai, China). Lipofectamine 3000 reagents

Figure 4. SKA3 is upregulated in LSCC and is linked to the malignant progression of LSCC

(A) SKA3 mRNA levels in 150 LSCC and matched ANM tissues were assayed by qPCR analysis. (B–E) Analysis of the relationship between SKA3 expression levels and T stages (B), lymph node metastasis (C), clinical stages (D), and pathological differentiation degree (E). (F and G) SKA3 protein levels in selected LSCC tissues and matched ANM tissues validated by IHC staining (F) and western blotting (G). Protein bands were quantified by ImageJ, and the relative expression of SKA3 in LSCC tissues (T) was calculated by normalizing to Tubulin and matched ANM tissues (N). Scale bars, 50 μm. (H) Expression of SKA3 in LSCC and HNSCC was analyzed with RNA-seq data from the TCGA database. (I) Kaplan-Meier assessment of the association of SKA3 levels with overall survival of patients with HNSCC. Expression and clinical data were from the TCGA database. (J) SKA3 expression levels in 32 other types of cancer from TCGA database plotted by GEPIA2 (http://gepia2.cancer-pku.cn/). (K) Kaplan-Meier survival inspection of the association of SKA3 expression levels with 32 types of cancer plotted by GEPIA2. For Kaplan-Meier analysis in (I) and (K), the expression levels of SKA3 were divided into low or high groups according to the median FPKM value.

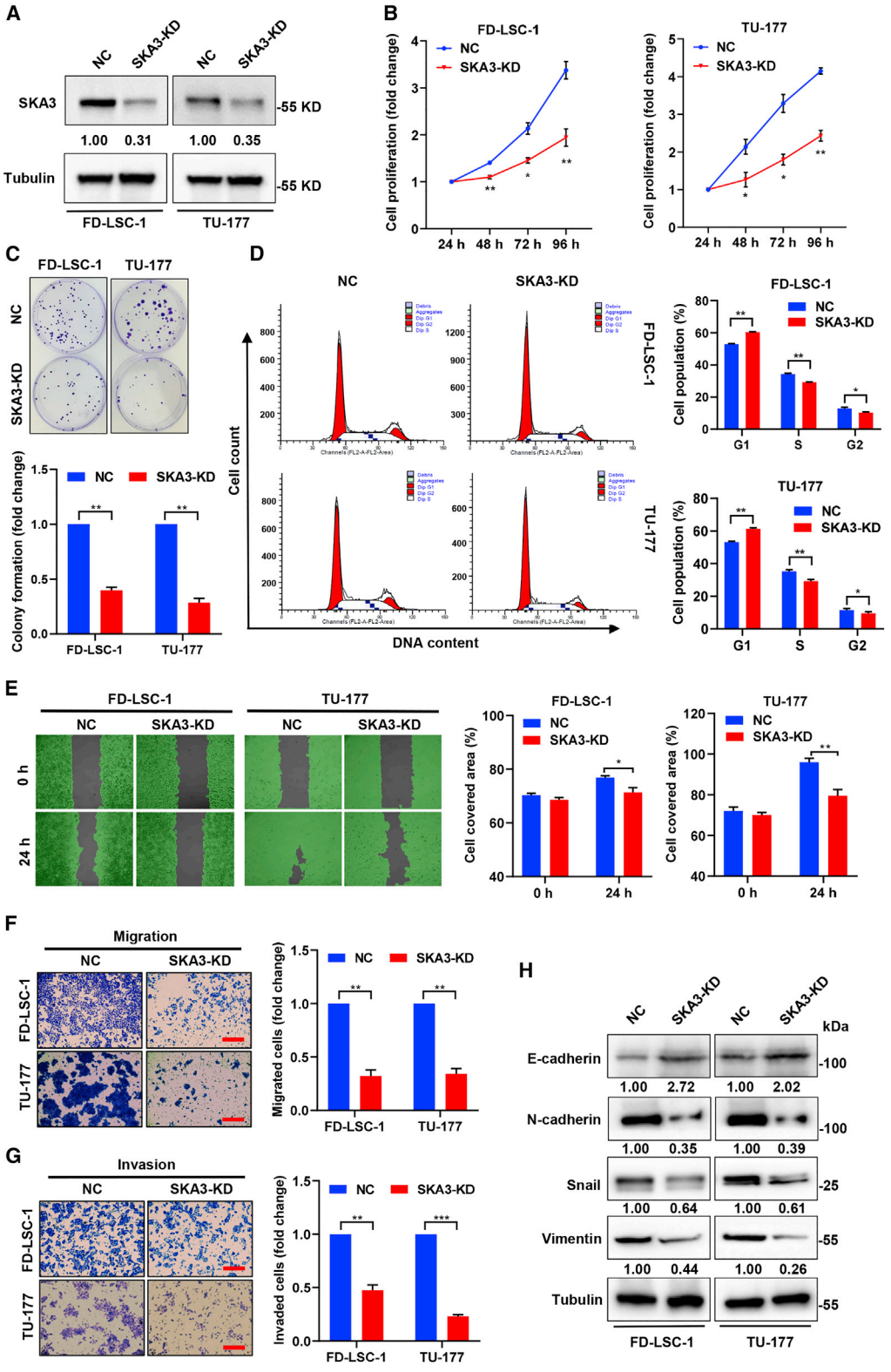

(legend on next page)

(Thermo Fisher Scientific) were used to transfect miRNA mimics, miRNA inhibitor, miRNA agomir, or siRNA according to the manufacturer's instructions. The si-SKA3 sequence is as follows: 5′-CCAC CUACCAAACAAUCACUA-3′; 5′-UAGUGAUUGUUUGGUAGG UGG-3′.

Gene expression analysis

TRIzol reagent (Invitrogen, USA) was used to isolate total RNA from cells or tissues. The RNA was reverse transcribed into cDNA with a cDNA synthesis kit (Thermo Fisher) and the miScript II RT Kit (QIAGEN, Germany) for mRNA and miRNA, respectively. The TransStart Tip Green qPCR SuperMix (Transgen Biotech) was used to perform qPCR on a LightCycler 96 instrument (Roche, Indianapolis, IN, USA) according to the manufacturer's protocol. The levels of U6 and Actin were used as internal controls. The primer sequences were as follows: *SKA3*: 5′-GCTCAGCATGGACCCTATCC-3′, 5′-TGGA TAATCTTCAAAGTCGCTTTCC-3′; *U6*: 5′-TCGCTTCGGCAGCA CATAT-3′, 5′-ATTTGCGTGTCATCCTTGC-3′; *Actin*: 5′-TCCC TGGAGAAGAGCTACGA-3′, 5′-AGCACTGTGTTGGCGTACAG-3′; miR-1207-5p forward: TGGCAGGGAGGCTGGGAGG. Tables S1 and S2 describe the clinical characteristics of the LSCC samples used for qPCR analysis.

Luciferase activity assay

WT or Mut *SKA3* reporter plasmid was co-transfected with NC/miR-1207-5p mimics/miR-1207-5p repressor for 48 h. The luciferase enzyme activity was assessed with the Dual-Luciferase enzyme Assay System (Promega, Madison, WI, USA) according to the manufacturer's instructions.

Western blot analysis

For protein extraction, we used radioimmunoprecipitation (RIPA) buffer containing a cocktail of protease inhibitors (Thermo Fisher Scientific). Subsequently, we resolved equal amounts of the protein on SDS-PAGE and transfer-embedded it onto polyvinylidene fluoride (PVDF) membranes (Millipore, Bedford, MA, USA). After blocking with 5% non-fat milk, the cells were incubated at 4°C overnight with primary antibodies, rinsed three times with Tris Buffered Saline with Tween 20 (TBST), and incubated with secondary antibodies at room temperature (RT) for 2 h. The protein bands were visualized with an enhanced chemiluminescence (ECL) reagent (ZETA LIFE). The primary antibodies anti-SKA3 (Cat# A304-215A, Bethyl Laboratories, Montgomery, TX, USA), anti-N-cadherin (Cat# 13116S, CST, Danvers, MA, USA), anti-Vimentin (Cat# 5741S, CST), anti-Snail (Cat# 3879S, CST), anti-E-cadherin (Cat# 3195S, CST), and anti-Tubulin (Cat# HC101, Transgen Biotech) were used in this study.

CCK8 and colony formation assays

For CCK8 analysis, cells (1×10^3 cells/well) were seeded into 96-well plates and incubated for the time indicated. The ability to proliferate was measured with a CCK8 kit (Yeasen, Shanghai, China) according to the manufacturer's protocol. For the colony formation experiment, cells were cultured in 35-mm dishes for 12 days and stained with crystal violet.

Wound healing assay

Cells were planted in Culture-Insert 2 Wells (ibidi, Fitchburg, WI, USA) according to the manufacturer's instructions, and wound recovery was observed at the indicated time points.

Transwell migration and invasion assay

The cells were suspended in a serum-free medium. Matrigel (BD Biosciences, San Jose, CA, USA) was used to precoat the Transwell chambers for the invasion experiment. In the upper chamber 100 μL of serum-free medium with cells (1×10^5 cells/well for invasion or 4×10^4 cells/well for migration) was introduced, and 600 μL of medium containing 20% FBS was introduced in the lower chamber. Cells in the upper chamber were cleaned, and the chamber was rinsed with PBS (Phosphate Buffered Saline) and fixed with paraformaldehyde. Cells were transferred to the lower chamber and stained with crystal violet and then observed and photographed with an inverted microscope (Leica Microsystems, Buffalo Grove, IL, USA).

In situ hybridization of miR-1207-5p

In situ hybridization of miR-1207-5p was performed as previously described[49] with miRCURY LNA miRNA ISH Optimization Kits (FFPE) (QIAGEN, Germantown, MD, USA) according to the manufacturer's instructions. Briefly, 6-μm-thick paraffin sections were dewaxed and rehydrated. Sections were digested for 20 min at 37°C with 15 μg/mL Proteinase K and then incubated with a 30 nM double DIG-labeled miR-1207-5p probe (QIAGEN, Germantown, MD, USA) for 1 h at 55 °C. Segments were incubated with sheep anti-DIG-AP (Roche) antibody at a concentration of 1:800 for 1 h at RT. For signal detection, sections were incubated with AP substrate for 2 h at 30°C, and then counterstaining was performed with Nuclear Fast Red (Vector Laboratories, Burlingame, CA, USA) for 1 min. The slides were mounted, examined, and photographed under a microscope. One double-(5′ and 3′)-DIG-labeled Scramble-miR probe was used as a negative control.

Immunohistochemical staining

IHC staining was performed as previously described.[5] Briefly, 3 μm of paraffin-embedded sections was prepared and dewaxed. Then,

Figure 5. SKA3 promotes the proliferation, cell cycle progression, migration, and invasion of LSCC cells

(A) LSCC cells were transfected with si-SKA3 (SKA3-KD) or NC siRNA for 48 h, and the expression of SKA3 was detected by western blot. Protein bands were quantified by ImageJ, and the relative expression was calculated by normalizing to Tubulin and NC arm. (B) The proliferation of SKA3 knockdown cells was assessed by CCK8 assay at the time points indicated. (C) Colony formation assay of SKA3 knockdown LSCC cells. (D) Cells were transfected with si-SKA3 and analyzed by flow cytometry to study the cell cycle. (E) Cells were transfected with si-SKA3, and wound healing assay was performed at the time points indicated. (F and G) Cells transfected with si-SKA3, and migration as well as invasive abilities were evaluated by Transwell assays. Scale bars, 200 μm. (H) Cells transfected with si-SKA3 for 48 h, and the levels of Vimentin, N-cadherin, E-cadherin, and Snail proteins were assessed by western blotting. Data are mean ± SD of three separate experiments. *$p < 0.05$ and **$p < 0.01$.

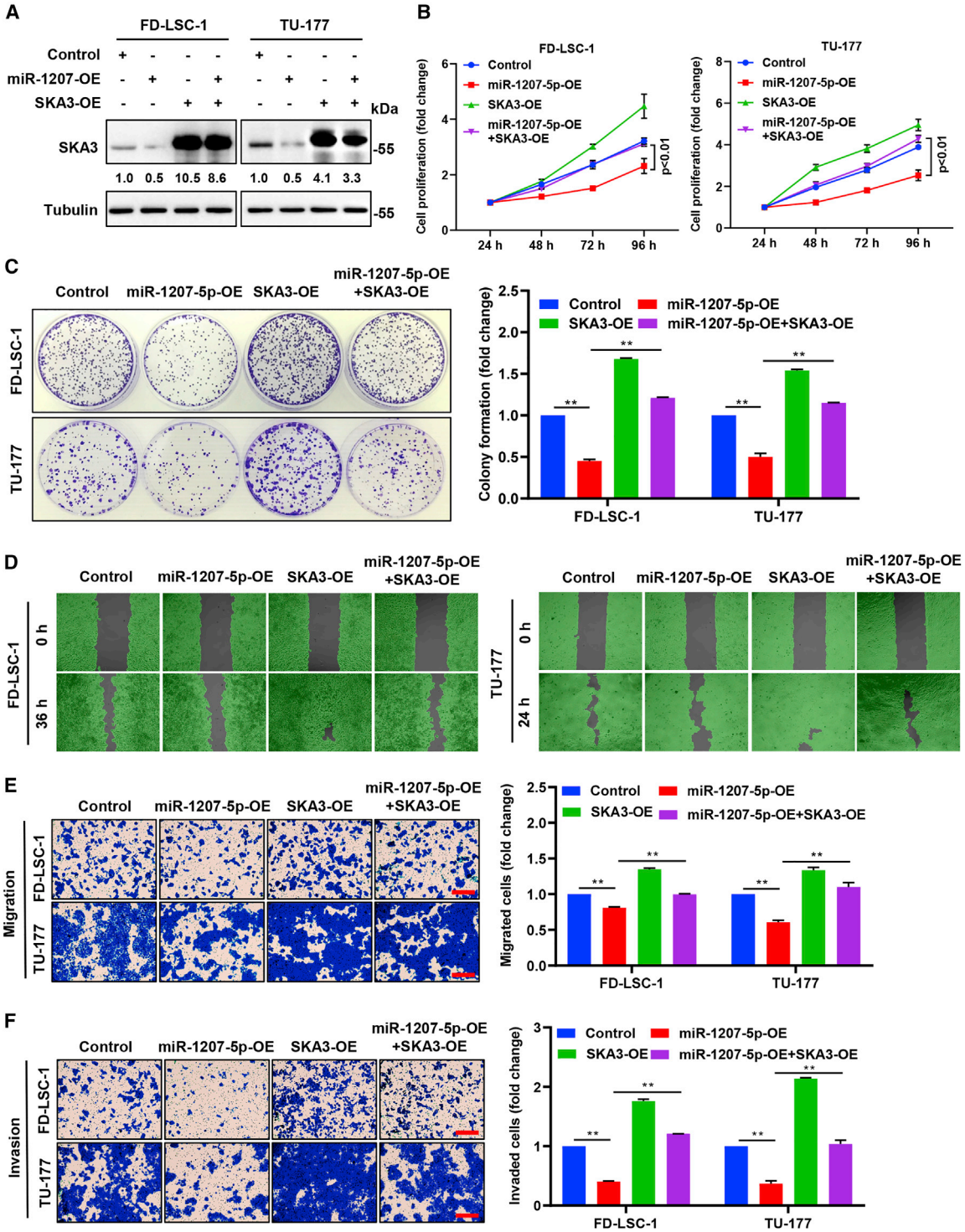

Figure 6. Overexpression of SKA3 reversed the tumor-inhibiting effects of miR-1207-5p in LSCC cells

TU-177 and FD-LSC-1 cells were transfected with miR-1207-5p mimics or SKA3 overexpression plasmid (SKA3-OE) or co-transfected with miR-1207-5p mimics and SKA3-OE via transfection. (A) The expression level of SKA3 was evaluated after 48 h of transfection by western blotting. Protein bands were quantified by ImageJ, and the relative expression was calculated by normalizing to Tubulin and Control arm. (B) Cell proliferation was assessed by CCK8 assay at the time points indicated. (C) Colony formation assay of LSCC cells. (D) Wound healing assay was conducted at the time points indicated. (E and F) Migration (E) and invasion (F) ability were determined by Transwell assays. Scale bars, 200 μm. Data are mean ± SD of three separate experiments. *$p < 0.05$ and **$p < 0.01$.

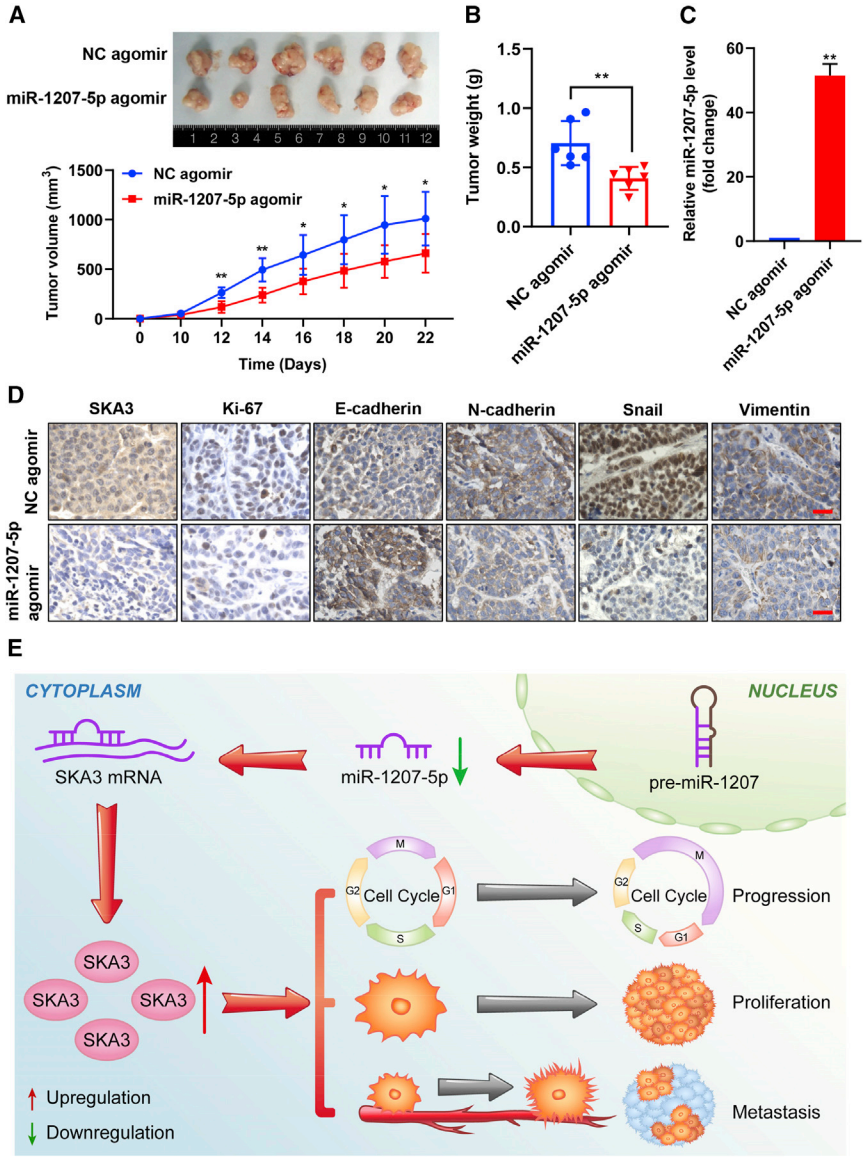

Figure 7. Effect of miR-1207-5p on tumor growth in a xenograft model

Nude mice were subcutaneously administered with TU-177 cells to construct a xenograft model. After tumor formation, miR-1207-5p agomir or negative control (NC) agomir was injected intratumor. (A) Representative images and growth curve of tumor at 12 days after injection of miR-1207-5p agomir or NC agomir in LSCC xenograft model. (B) The xenograft tumor weight was measured and plotted at 12 days after injection. (C) miR-1207-5p expression in xenograft tumors validated by qPCR. (D) The expression changes of SKA3, Ki-67, E-cadherin, N-cadherin, Snail, and Vimentin in xenograft tumors were examined by IHC staining. Representative images are shown. Scale bars, 25 μm. *$p < 0.05$ and **$p < 0.01$. Data are mean ± SD of three separate experiments. (E) Schematic model depicting that miR-1207-5p/SKA3 signaling axis regulates LSCC progression.

re-hydration, antigen retrieval, blocking, and incubation with primary antibodies at 4°C overnight were performed. The sections were then incubated with the secondary antibody for 0.5 h at RT and stained before being stained with 3,3′-diaminobenzidine (DAB) solution and hematoxylin. Finally, the sections were dehydrated and covered with coverslips.

Xenograft model studies

BALB/c nude mice (female, aged 6 weeks) were obtained from Beijing Vital River Laboratory Animal Technology (Beijing, China). TU-177 cells (2×10^6 cells/mouse) were administered subcutaneously into each mouse's right flank. A total of 12 mice were inoculated, and 10 days later xenograft models were randomized into 2 arms (n = 6), six mice receiving 10 nmol NC agomir intratumor and the other six mice receiving miR-1207-5p agomir. Tumor-bearing mice were anesthetized with isoflurane and euthanized via cervical dislocation on day 22, and the xenograft tumors were dissected, weighed, and photographed.

Cell cycle assay

A Cell Cycle and Apoptosis Analysis Kit was used to measure the cell cycle (Beyotime, Shanghai, China). In brief, cells were digested, rinsed with PBS, and then fixated with ethanol (70%) overnight at 4°C. The cells were then centrifuged, rinsed with PBS, resuspended with 0.5 mL of propidium solution, and analyzed on a NovoCyte flow cytometer (ACEA, Hangzhou, China).

Bioinformatics analysis

The normalized expression data fragments per kilobase million (FPKM) of an HNSCC cohort retrieved from TCGA were used for differential expression and Kaplan-Meier analysis for SKA3 in HNSCC survival and expression analysis. The web server GEPIA2 (http://gepia2.cancer-pku.cn/) was used to analyze SKA3 survival and expression in 32 different types of cancer. TargetscanHuman 7.1 was used to predict miR-1207-5p target genes.[50] DAVID 6.8 (https://david.ncifcrf.gov/) was used to perform GO and KEGG pathway annotation.[51]

Statistical analyses

Statistical analyses were carried out with GraphPad 8 software. Data are presented as the mean ± standard deviation (SD). The unpaired t test was used to determine the relative differences between the two arms. Overall survival was defined as the time from the date of surgery to the date of death from laryngeal carcinoma or the last follow-up date. Survival analysis was carried out with the Kaplan-Meier method. $p < 0.05$ was considered statistically significant.

SUPPLEMENTAL INFORMATION

Supplemental information can be found online at https://doi.org/10.1016/j.omto.2021.08.001.

ACKNOWLEDGMENTS

This work was supported by the National Natural Science Foundation of China (Nos. 81872210, 81802948, and 82073101), The Excellent talent science and technology innovation project of Shanxi Province (Nos. 201605D211029, 201705D211018, and 201805D211007), the Research Funds for China Central Government-guided Development of Local Science and Technology (No. 2020-165-19), Shanxi Province Scientific and Technological Achievements Transformation Guidance Foundation (No. 201804D131043), Shenzhen Key Laboratory Foundation (No. ZDSYS20200811143757022), Shanxi Province Science Foundation for Excellent Young Scholars (No. 201901D211486), Applied Basic Research project of Shanxi province (Nos. 201801D221421 and 201901D211490), Youth Foundation of The First Hospital Affiliated with Shanxi Medical University (No. YQ1503), Youth Top Talent Program Fund of Shanxi Province, Fund of Shanxi "1331" Project, Open Fund from Key Laboratory of Cellular Physiology (Shanxi Medical University), and Ministry of Education, China (Nos. KLMEC/SXMU-202008 and KLMEC/SXMU-202009).

AUTHOR CONTRIBUTIONS

W.G. and J.C. performed the conception and design. Y.W. and F.D. were involved in the development of methodology. Y.W., F.D., Y.Z., and L.L. performed most of the experiments and were involved in the acquisition of data. Y.W., F.D., and Y.Z. were involved in the analysis and interpretation of data. X.Z. performed bioinformatics analysis. Y.W. and F.D. were involved in figure organization. Y.W., F.D., and W.G. wrote, reviewed, and revised the manuscript. W.G. and J.C. were involved in the study supervision.

DECLARATION OF INTERESTS

The authors declare no competing interests.

REFERENCES

1. Ekizoglu, S., Seven, D., Ulutin, T., Guliyev, J., and Buyru, N. (2018). Investigation of the SLC22A23 gene in laryngeal squamous cell carcinoma. BMC Cancer *18*, 477.
2. Steuer, C.E., El-Deiry, M., Parks, J.R., Higgins, K.A., and Saba, N.F. (2017). An update on larynx cancer. CA Cancer J. Clin. *67*, 31–50.
3. Anschuetz, L., Shelan, M., Dematté, M., Schubert, A.D., Giger, R., and Elicin, O. (2019). Long-term functional outcome after laryngeal cancer treatment. Radiat. Oncol. *14*, 101.
4. Kostrzewska-Poczekaj, M., Byzia, E., Soloch, N., Jarmuz-Szymczak, M., Janiszewska, J., Kowal, E., Paczkowska, J., Kiwerska, K., Wierzbicka, M., Bartochowska, A., et al. (2019). DIAPH2 alterations increase cellular motility and may contribute to the metastatic potential of laryngeal squamous cell carcinoma. Carcinogenesis *40*, 1251–1259.
5. Gao, W., Zhang, C., Li, W., Li, H., Sang, J., Zhao, Q., Bo, Y., Luo, H., Zheng, X., Lu, Y., et al. (2019). Promoter Methylation-Regulated miR-145-5p Inhibits Laryngeal Squamous Cell Carcinoma Progression by Targeting FSCN1. Mol. Ther. *27*, 365–379.
6. Kompelli, A.R., Li, H., and Neskey, D.M. (2019). Impact of Delay in Treatment Initiation on Overall Survival in Laryngeal Cancers. Otolaryngol. Head Neck Surg. *160*, 651–657.
7. Yang, D., Shi, Y., Tang, Y., Yin, H., Guo, Y., Wen, S., Wang, B., An, C., Wu, Y., and Gao, W. (2019). Effect of HPV Infection on the Occurrence and Development of Laryngeal Cancer: A Review. J. Cancer *10*, 4455–4462.
8. Gao, W., Zhang, Y., Luo, H., Niu, M., Zheng, X., Hu, W., Cui, J., Xue, X., Bo, Y., Dai, F., et al. (2020). Targeting SKA3 suppresses the proliferation and chemoresistance of laryngeal squamous cell carcinoma via impairing PLK1-AKT axis-mediated glycolysis. Cell Death Dis. *11*, 919.
9. Wu, Y., Zhang, Y., Zheng, X., Dai, F., Lu, Y., Dai, L., Niu, M., Guo, H., Li, W., Xue, X., et al. (2020). Circular RNA circCORO1C promotes laryngeal squamous cell carcinoma progression by modulating the let-7c-5p/PBX3 axis. Mol. Cancer *19*, 99.
10. Gao, W., Guo, H., Niu, M., Zheng, X., Zhang, Y., Xue, X., Bo, Y., Guan, X., Li, Z., Guo, Y., et al. (2020). circPARD3 drives malignant progression and chemoresistance of laryngeal squamous cell carcinoma by inhibiting autophagy through the PRKCI-Akt-mTOR pathway. Mol. Cancer *19*, 166.
11. Li, X., Xu, F., Meng, Q., Gong, N., Teng, Z., Xu, R., Zhao, M., and Xia, M. (2020). Long noncoding RNA DLEU2 predicts a poor prognosis and enhances malignant properties in laryngeal squamous cell carcinoma through the miR-30c-5p/PIK3CD/Akt axis. Cell Death Dis. *11*, 472.
12. Zhao, Q., Zheng, X., Guo, H., Xue, X., Zhang, Y., Niu, M., Cui, J., Liu, H., Luo, H., Yang, D., et al. (2020). Serum Exosomal miR-941 as a promising Oncogenic Biomarker for Laryngeal Squamous Cell Carcinoma. J. Cancer *11*, 5329–5344.
13. Bartel, D.P. (2018). Metazoan MicroRNAs. Cell *173*, 20–51.
14. Luo, Y., Wu, J., Wu, Q., Li, X., Wu, J., Zhang, J., Rong, X., Rao, J., Liao, Y., Bin, J., et al. (2019). miR-577 Regulates TGF-β Induced Cancer Progression through a SDPR-Modulated Positive-Feedback Loop with ERK-NF-κB in Gastric Cancer. Mol. Ther. *27*, 1166–1182.
15. Yu, Y., Yin, W., Yu, Z.H., Zhou, Y.J., Chi, J.R., Ge, J., and Cao, X.C. (2019). miR-190 enhances endocrine therapy sensitivity by regulating SOX9 expression in breast cancer. J. Exp. Clin. Cancer Res. *38*, 22.
16. Wang, S.N., Luo, S., Liu, C., Piao, Z., Gou, W., Wang, Y., Guan, W., Li, Q., Zou, H., Yang, Z.Z., et al. (2017). miR-491 Inhibits Osteosarcoma Lung Metastasis and Chemoresistance by Targeting αB-crystallin. Mol. Ther. *25*, 2140–2149.
17. Yang, C., Ma, X., Guan, G., Liu, H., Yang, Y., Niu, Q., Wu, Z., Jiang, Y., Bian, C., Zang, Y., and Zhuang, L. (2019). MicroRNA-766 promotes cancer progression by targeting NR3C2 in hepatocellular carcinoma. FASEB J. *33*, 1456–1467.
18. Zhao, X., Zhang, W., and Ji, W. (2018). miR-196b is a prognostic factor of human laryngeal squamous cell carcinoma and promotes tumor progression by targeting SOCS2. Biochem. Biophys. Res. Commun. *501*, 584–592.
19. Li, P., Lin, X.J., Yang, Y., Yang, A.K., Di, J.M., Jiang, Q.W., Huang, J.R., Yuan, M.L., Xing, Z.H., Wei, M.N., et al. (2019). Reciprocal regulation of miR-1205 and E2F1 modulates progression of laryngeal squamous cell carcinoma. Cell Death Dis. *10*, 916.
20. Zhang, C., Gao, W., Wen, S., Wu, Y., Fu, R., Zhao, D., Chen, X., and Wang, B. (2016). Potential key molecular correlations in laryngeal squamous cell carcinoma revealed by integrated analysis of mRNA, miRNA and lncRNA microarray profiles. Neoplasma *63*, 888–900.
21. Gonzalez, D.M., and Medici, D. (2014). Signaling mechanisms of the epithelial-mesenchymal transition. Sci. Signal. *7*, re8.
22. Daum, J.R., Wren, J.D., Daniel, J.J., Sivakumar, S., McAvoy, J.N., Potapova, T.A., and Gorbsky, G.J. (2009). Ska3 is required for spindle checkpoint silencing and the maintenance of chromosome cohesion in mitosis. Curr. Biol. *19*, 1467–1472.
23. Hou, Y., Wang, Z., Huang, S., Sun, C., Zhao, J., Shi, J., Li, Z., Wang, Z., He, X., Tam, N.L., and Wu, L. (2019). SKA3 Promotes tumor growth by regulating CDK2/P53 phosphorylation in hepatocellular carcinoma. Cell Death Dis. *10*, 929.
24. Hu, R., Wang, M.Q., Niu, W.B., Wang, Y.J., Liu, Y.Y., Liu, L.Y., Wang, M., Zhong, J., You, H.Y., Wu, X.H., et al. (2018). SKA3 promotes cell proliferation and migration in cervical cancer by activating the PI3K/Akt signaling pathway. Cancer Cell Int. *18*, 183.
25. Chen, Y., Song, Y., Mi, Y., Jin, H., Cao, J., Li, H., Han, L., Huang, T., Zhang, X., Ren, S., et al. (2020). microRNA-499a promotes the progression and chemoresistance of cervical cancer cells by targeting SOX6. Apoptosis *25*, 205–216.
26. Kulkarni, B., Kirave, P., Gondaliya, P., Jash, K., Jain, A., Tekade, R.K., and Kalia, K. (2019). Exosomal miRNA in chemoresistance, immune evasion, metastasis and progression of cancer. Drug Discov. Today *24*, 2058–2067.

27. Lee, J.W., Guan, W., Han, S., Hong, D.K., Kim, L.S., and Kim, H. (2018). MicroRNA-708-3p mediates metastasis and chemoresistance through inhibition of epithelial-to-mesenchymal transition in breast cancer. Cancer Sci. *109*, 1404–1413.

28. Wu, Y., Zhang, Y., Niu, M., Shi, Y., Liu, H., Yang, D., Li, F., Lu, Y., Bo, Y., Zhang, R., et al. (2018). Whole-Transcriptome Analysis of CD133+CD144+ Cancer Stem Cells Derived from Human Laryngeal Squamous Cell Carcinoma Cells. Cell. Physiol. Biochem. *47*, 1696–1710.

29. Zhang, Y., Chen, Y., Yu, J., Liu, G., and Huang, Z. (2014). Integrated transcriptome analysis reveals miRNA-mRNA crosstalk in laryngeal squamous cell carcinoma. Genomics *104*, 249–256.

30. Yang, X., Zang, W., Xuan, X., Wang, Z., Liu, Z., Wang, J., Cui, J., and Zhao, G. (2015). miRNA-1207-5p is associated with cancer progression by targeting stomatin-like protein 2 in esophageal carcinoma. Int. J. Oncol. *46*, 2163–2171.

31. Zhao, G., Dong, L., Shi, H., Li, H., Lu, X., Guo, X., and Wang, J. (2016). MicroRNA-1207-5p inhibits hepatocellular carcinoma cell growth and invasion through the fatty acid synthase-mediated Akt/mTOR signalling pathway. Oncol. Rep. *36*, 1709–1716.

32. Xu, G., Zhu, Y., Liu, H., Liu, Y., and Zhang, X. (2020). LncRNA MIR194-2HG Promotes Cell Proliferation and Metastasis via Regulation of miR-1207-5p/TCF19/Wnt/β-Catenin Signaling in Liver Cancer. OncoTargets Ther. *13*, 9887–9899.

33. Lü, M.H., Tang, B., Zeng, S., Hu, C.J., Xie, R., Wu, Y.Y., Wang, S.M., He, F.T., and Yang, S.M. (2016). Long noncoding RNA BC032469, a novel competing endogenous RNA, upregulates hTERT expression by sponging miR-1207-5p and promotes proliferation in gastric cancer. Oncogene *35*, 3524–3534.

34. Yan, Y., Su, M., and Qin, B. (2020). CircHIPK3 promotes colorectal cancer cells proliferation and metastasis via modulating of miR-1207-5p/FMNL2 signal. Biochem. Biophys. Res. Commun. *524*, 839–846.

35. Hou, X., Niu, Z., Liu, L., Guo, Q., Li, H., Yang, X., and Zhang, X. (2019). miR-1207-5p regulates the sensitivity of triple-negative breast cancer cells to Taxol treatment via the suppression of LZTS1 expression. Oncol. Lett. *17*, 990–998.

36. Yan, C., Chen, Y., Kong, W., Fu, L., Liu, Y., Yao, Q., and Yuan, Y. (2017). PVT1-derived miR-1207-5p promotes breast cancer cell growth by targeting STAT6. Cancer Sci. *108*, 868–876.

37. Guimaraes, G.J., and Deluca, J.G. (2009). Connecting with Ska, a key complex at the kinetochore-microtubule interface. EMBO J. *28*, 1375–1377.

38. Theis, M., Paszkowski-Rogacz, M., and Buchholz, F. (2009). SKAnking with Ska3: essential role of Ska3 in cell division revealed by combined phenotypic profiling. Cell Cycle *8*, 3435–3437.

39. Pastushenko, I., and Blanpain, C. (2019). EMT Transition States during Tumor Progression and Metastasis. Trends Cell Biol. *29*, 212–226.

40. Zheng, X., Carstens, J.L., Kim, J., Scheible, M., Kaye, J., Sugimoto, H., Wu, C.C., LeBleu, V.S., and Kalluri, R. (2015). Epithelial-to-mesenchymal transition is dispensable for metastasis but induces chemoresistance in pancreatic cancer. Nature *527*, 525–530.

41. Zhou, P., Li, B., Liu, F., Zhang, M., Wang, Q., Liu, Y., Yao, Y., and Li, D. (2017). The epithelial to mesenchymal transition (EMT) and cancer stem cells: implication for treatment resistance in pancreatic cancer. Mol. Cancer *16*, 52.

42. Xu, E., Xia, X., Jiang, C., Li, Z., Yang, Z., Zheng, C., Wang, X., Du, S., Miao, J., Wang, F., et al. (2020). GPER1 Silencing Suppresses the Proliferation, Migration, and Invasion of Gastric Cancer Cells by Inhibiting PI3K/AKT-Mediated EMT. Front. Cell Dev. Biol. *8*, 591239.

43. Tian, J., Zhang, H., Mu, L., Wang, M., Li, X., Zhang, X., Xie, E., Ma, M., Wu, D., and Du, Y. (2020). The miR-218/GAB2 axis regulates proliferation, invasion and EMT via the PI3K/AKT/GSK-3β pathway in prostate cancer. Exp. Cell Res. *394*, 112128.

44. Wang, B., Wang, L., Lu, Y., Liang, W., Gao, Y., Xi, H., and Chen, L. (2021). GRSF1 promotes tumorigenesis and EMT-mediated metastasis through PI3K/AKT pathway in gastric cancer. Biochem. Biophys. Res. Commun. *555*, 61–66.

45. Nan, Y., Guo, L., Lu, Y., Guo, G., Hong, R., Zhao, L., Wang, L., Ren, B., Yu, K., Zhong, Y., and Huang, Q. (2021). miR-451 suppresses EMT and metastasis in glioma cells. Cell Cycle *20*, 1270–1278.

46. Hu, D.D., Chen, H.L., Lou, L.M., Zhang, H., and Yang, G.L. (2020). SKA3 promotes lung adenocarcinoma metastasis through the EGFR-PI3K-Akt axis. Biosci. Rep. *40*, BSR20194335.

47. Wang, W., Zhang, L., Wang, Y., Ding, Y., Chen, T., Wang, Y., Wang, H., Li, Y., Duan, K., Chen, S., et al. (2017). Involvement of miR-451 in resistance to paclitaxel by regulating YWHAZ in breast cancer. Cell Death Dis. *8*, e3071.

48. Wu, C.P., Zhou, L., Gong, H.L., Du, H.D., Tian, J., Sun, S., and Li, J.Y. (2014). Establishment and characterization of a novel HPV-negative laryngeal squamous cell carcinoma cell line, FD-LSC-1, with missense and nonsense mutations of TP53 in the DNA-binding domain. Cancer Lett. *342*, 92–103.

49. Conserva, F., Barozzino, M., Pesce, F., Divella, C., Oranger, A., Papale, M., Sallustio, F., Simone, S., Laviola, L., Giorgino, F., et al. (2019). Urinary miRNA-27b-3p and miRNA-1228-3p correlate with the progression of Kidney Fibrosis in Diabetic Nephropathy. Sci. Rep. *9*, 11357.

50. Agarwal, V., Bell, G.W., Nam, J.W., and Bartel, D.P. (2015). Predicting effective microRNA target sites in mammalian mRNAs. eLife *4*, e05005.

51. Huang, D.W., Sherman, B.T., and Lempicki, R.A. (2009). Systematic and integrative analysis of large gene lists using DAVID bioinformatics resources. Nat. Protoc. *4*, 44–57.